IEEE Access
Multidisciplinary | Rapid Review | Open Access Journal

Received September 21, 2020, accepted October 15, 2020, date of publication October 19, 2020, date of current version November 3, 2020.

Digital Object Identifier 10.1109/ACCESS.2020.3032163

Development and Field Test of Unmanned Marine Vehicle (USV/UUV) With cable

SUNG MIN HONG[1], (Member, IEEE), KEON SEOK NAM[1], JE DOO RYU[1], DONG GU LEE[1], AND KYOUNG NAM HA[1], (Member, IEEE)
Marine Robot Center, Korea Institute of Industrial Technology, Busan 46041, South Korea

Corresponding author: Kyoung Nam Ha (0vincent@kitech.re.kr)

This work was supported by the Korea Institute of Industrial Technology as The Development of Intelligent Marine Robot to Improve Underwater Work Convenience under Grant kitech JA-20-0002.

ABSTRACT This paper presents the system, controller, and field test results of an unmanned marine vehicle (UMV) developed to acquire real-time ocean exploration information. The system consists of an unmanned surface vehicle (USV), an unmanned underwater vehicle (UUV), and an underwater cable. The developed platform is a research platform for ocean exploration and was proposed to compensate for the shortcomings of the existing USV, UUV, and towing system. This paper describes the proposed UMV, including the design considerations such as electronics architecture, data management, sensors, and actuators and explains the path control algorithm and controller used to follow the specified path for ocean exploration. In order to confirm the performance of the developed platform and control algorithm, a way-point tracking experiment was performed, and the results are shown.

INDEX TERMS Unmanned surface vehicle, unmanned underwater vehicle, leader-follower method, pure-pursuit method, anti-windup controller, field test.

I. INTRODUCTION

Ocean exploration is essential in various fields such as obtaining ocean environment data, developing marine resources and energy, maritime safety, and military operations. Expansive investigation of the sea requires extensive resources: human, time and money. Furthermore, compared to working on land and in the air, working underwater is challenging to predict environmental changes, and the underwater environment raises many risks and limitations for humans directly performing the work. Therefore, scientists and technicians have tried to research and develop various automated systems and robotic equipment. Systems designed for ocean exploration can be divided into manned and unmanned.

The manned system uses a ship or mounts a towed system on a mother ship: it offers the advantage of being able to explore a large area for a long time but still requires considerable cost and human resources, and cannot be used to explore narrow or shallow waters. For the operation of the towed system, a constant speed of the mother ship is required. It is also difficult to predict the depth and attitude of the towed system in the event of a turning movement or displacement of the mother ship, and to determine the exact location of the exploration area.

The associate editor coordinating the review of this manuscript and approving it for publication was Yanli Xu.

The unmanned system was developed to conduct ocean exploration on behalf of humans and includes an unmanned surface vehicle (USV), remotely operated vehicle (ROV), autonomous underwater vehicle (AUV), and underwater glider (UG). The USV is capable of real-time communication with operators and can quickly explore vast areas, but may be difficult to operate depending on the sea state. ROV is used for work and exploration in a certain range, but it isn't easy to explore a large area because it is connected to an underwater cable and requires a mother ship. The AUV is capable of moving quickly and exploring a large area, but has the disadvantage of accumulating position errors over time, limited operating time depending on the battery's capacity, and impossible real-time communication. UG is capable of long-distance, long-term travel using buoyancy engines and moving mass system. But it is only suitable for acquiring seawater information such as temperature, density, and salinity by depth, not for obtaining topographic data of the exploration area.

Recently, as the technology of unmanned systems has been developed, research and platform development has been conducted to attempt ocean exploration by combining different platforms. The developed platform is shown in Figure 1.

SUBSEA TECH and MARINE TECH have developed CAT-Surveyor and RSV Sea Observer, respectively, which can be operated by combining a USV and ROV.

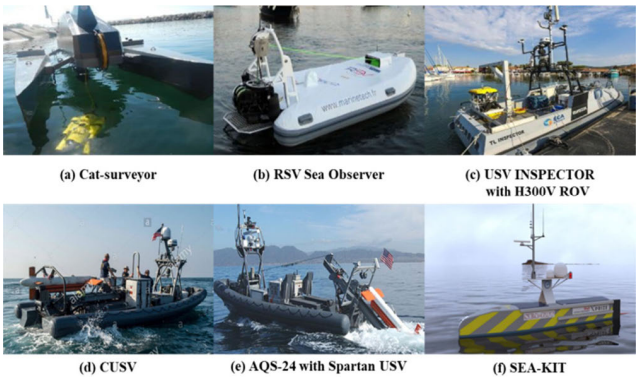

FIGURE 1. Unmanned Marine Platform combining heterogeneous system (USV-ROV & USV-Towed System).

The developed platform acquires hydrographic data or performs underwater inspection of the port area using a mounted sensor and camera. ECA GROUP is operated with H300V (ROV) installed in INSPECTOR (USV). This platform is used for underwater structure inspection and maintenance, and the manipulator mounted on the H300V is operated through remote control. TEXTRON Systems and Northrop Grumman developed CUSV and Spartan USV using a USV and a towed system, respectively. Spartan USV collaborated with the Naval Undersea Warfare Center in the United States to conduct a military purpose study to find underwater mines [1]–[11].

The above-described USV and ROV or towed system combined platform was developed for military purposes such as marine surveillance and inspection. Therefore, the information and technology of the platform have not been disclosed. However, by analogy, considering each platform's characteristics, the USV and ROV operation are limited to a restricted area of exploration. When operating a towed system, a speed more significant than a certain amount of the USV is required, and positional errors and attitudes of towed system instability during turning may introduce uncertainty in exploration information.

Therefore, this study proposes a combined USV and torpedo-type UUV platform to overcome the disadvantages of the existing platforms for ocean exploration. The USV was developed using a rubber boat and is responsible for power supply using large-capacity batteries and operator communication. The torpedo-type of UUV hull was manufactured to reduce water drag, and it was equipped with a thruster to enable straight forward and turn movements. Unlike ROV, it is possible to explore a wide area, and the position error that occurs when the USV turns, which is a disadvantage of the towed system, can be reduced through control. Using the USBL sensor, the USV and UUV can measure the relative position and the relative heading angle in order to reduce the accumulated error that may occur using inertial navigation. It is possible to maintain a formation as the relative position control is possible. This paper introduces the USV and UUV systems, including hardware systems, electronic architecture, data management, sensor, and actuator, explains the USV's

FIGURE 2. Unmanned Marine Vehicle (UMV) System configuration.

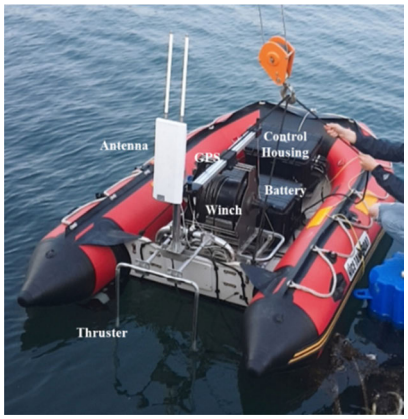

FIGURE 3. Assembled USV and components.

waypoint tracking and path control algorithms for moving a specified path for ocean exploration and describes the UUV control techniques for maintaining a constant distance from the USV and controlling the relative heading angle. To confirm the developed platform and control algorithm's performance, a waypoint control experiment was performed in the sea, and the results are presented.

II. CONFIGURATION OF THE UNMANNED MARINE VEHICLE (UMV)

The Unmanned Marine Vehicle (UMV) developed in this study is shown in Figure 2. The UMV consists of a USV, UUV and underwater cable, and the system includes a land-based operating console.

A. SYSTEM CONFIGURATION OF THE USV

In the UMV, the USV communicates with operators, supplies power to UUVs, operates the winch system, and tracks via waypoints. The developed USV is shown in Figure 3, and the specifications are presented in Table 1.

The USV was manufactured using a commercial rubber boat, and the installed equipment includes control housing, battery, communication equipment, winch, thrusters, GPS, and USBL ponder. In addition to measuring the position of the

TABLE 1. Specification of the USV.

Parameter	Value
Size (L x W x H)	3.00 m x 1.62 m x 0.47 m
Battery Capacity	Li-Po / 24V 400A
Thruster	Minn Kota (RT-80/EM) / Max. Force 36.2kfg
GPS	Hemisphere H200
AHRS	Xsens MTi-30
AP Bridge	GT-Wave
Controller	CY8CKIT-059 PSoC

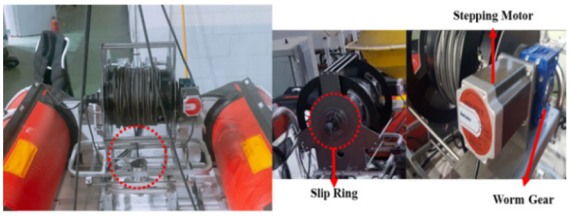

FIGURE 4. Winch system.

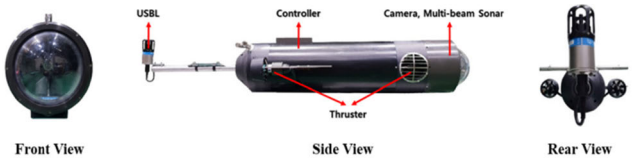

FIGURE 5. Assembled UUV and components.

USV, the GPS was able to measure the direction of the USV by installing two antennas. Figure 4 shows the winch system for launching and recovering the UUV and the holes drilled in the bottom of the USV to allow the underwater cable to move. The drum of the winch system was designed considering the radius of curvature of the underwater cable, and slip rings were used to prevent twisting of the cable.

B. SYSTEM CONFIGURATION OF THE UUV

The UUV conducts underwater exploration using sonar and a camera. The torpedo-type hull is made of aluminum 6061. The direction and position are controlled by attaching a thruster to the bow and aft. The UUV does not have a separate thruster for depth control and the depth is maintained using negative buoyancy. The USBL transceiver enables the relative position and direction to be measured with the USV. The underwater data, position, and attitude of the UUV are sent to the hub of the USV using an Ethernet communication. Figure 5 shows the developed UUV, and Table 2 presents the specification.

C. OPERATING SYSTEM

The console developed for operating the platform was manufactured using a commercial PC, and in case of emergency, an Xbox wireless controller is included for remote control.

The operation program was developed using LabView to display the attitude and position of the UMV and is divided into a remote control mode and an autonomous control mode. It is also has a command transmission component part and a component to check whether the platform is operating normally.

TABLE 2. Specification of the UUV.

Parameter	Value
Size (L x W x H)	1.79 m x 0.25 m x 0.25 m
Weight (in air)	36kgf
Thruster	Technadyne Model 300
Sonar	Oculus M750
AHRS	Xsens MTi-30
Depth Sensor	Sensys PSC
Controller	CY8CKIT-059 PSoC

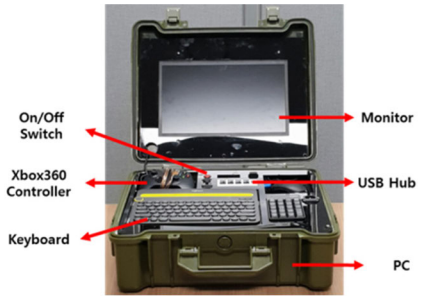

FIGURE 6. Operating console.

D. CONTROL SYSTEM

Figure 8 shows the control system configuration diagram of the UMV. The USV and UUV are composed of MCU1 for processing sensor data and MCU2 for calculation and output for the control algorithm. The USV's MCU1 receives commands and control gain from the operation console. The system is configured to transmit the information required for the UUV through an underwater cable.

III. GUIDANCE AND CONTROL FOR WAY-POINT TRACKING

Ocean exploration is mainly carried out by traveling along a predetermined path. Therefore, in this study, each platform's guidance and control method was designed to control the waypoint tracking of the UMV. The USV acts as a leader to follow a given waypoint and the desired values for control are calculated using the pure-pursuit method. The UUV acts as a follower to follow the USV and calculates the desired values using each platform's geometric relationship. An anti-windup PID controller was applied to obtain input for the thrusters using desired values obtained through each method and the information measured by a sensor. Figure 9 shows each platform's control scheme and this chapter introduces each control algorithm and controller.

A. PURE-PURSUIT METHOD FOR THE USV

In general, the path tracking method defines the distance between the current USV position from the reference path

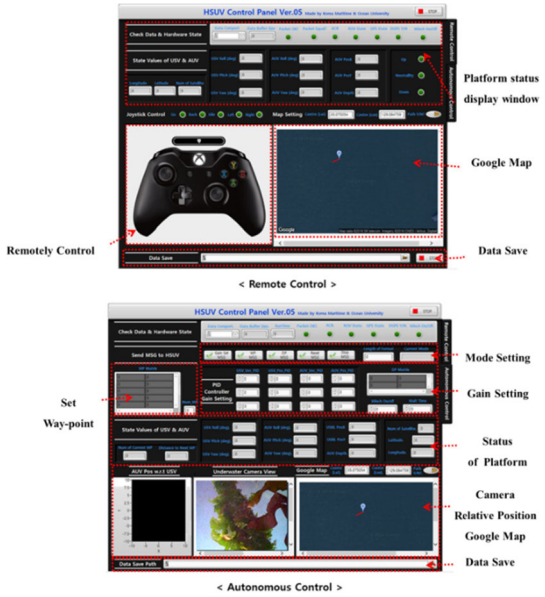

FIGURE 7. Operating program front panel.

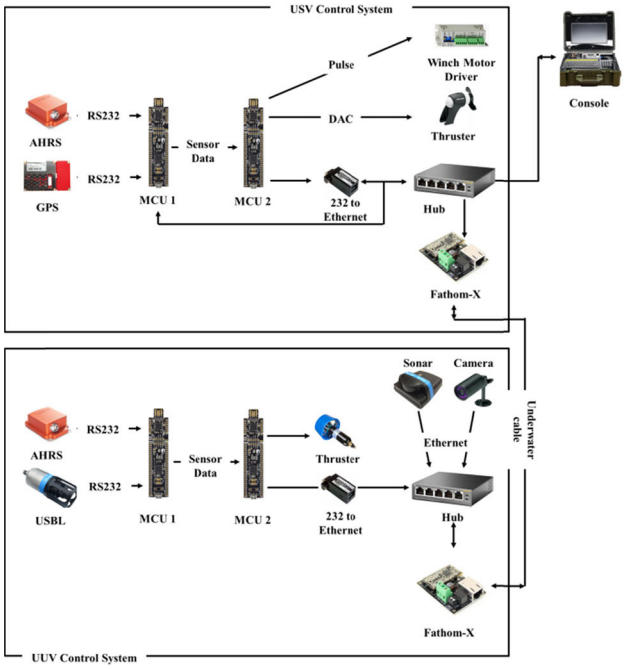

FIGURE 8. Control system of the UMV.

and the difference between the direction of the reference path and the heading angle of the USV as a position error and a heading angle error, respectively. The path is tracked through the control to reduce the defined error. Among various geometrical path tracking methods, the Pure-Pursuit method was used to select the look-ahead point for path tracking by obtaining the turning radius for tracking the path [12]–[14]. Figure 10 shows the process of returning the USV to the reference path by using the Pure-Pursuit method.

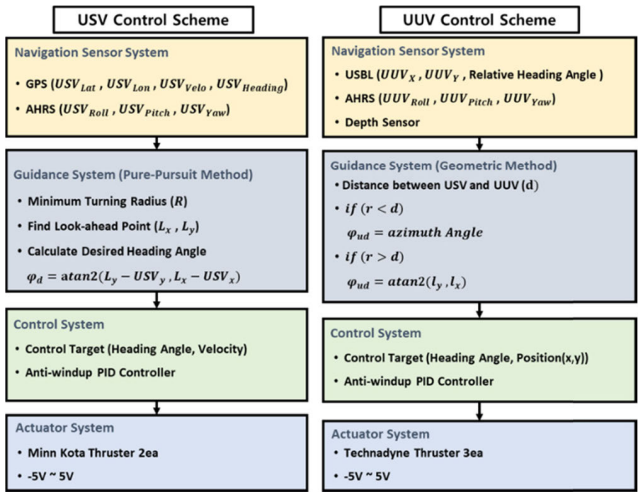

FIGURE 9. Control scheme of the UMV.

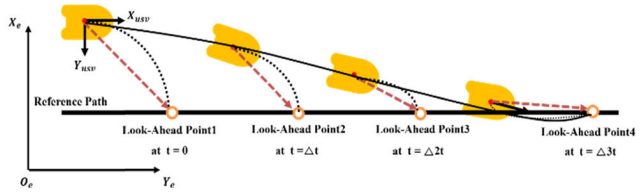

FIGURE 10. Pure pursuit method diagram.

The path given to the USV can be divided into a continuous path or a set of discontinuous waypoints. In the case of continuously representing a path, the path must be defined as a function on a two-dimensional plane, which results in the unnecessary calculation when applied to real hardware. Therefore, in this study, a path was defined using a set of discontinuous waypoints.

The geometric relationship can be defined using the following equations (1), (2) and (3) to find the turning radius of the USV, as shown in figure 11.

$$d^2 + b^2 = l^2 \tag{1}$$

$$a^2 + b^2 = R^2 \tag{2}$$

$$a = R - d \tag{3}$$

Substituting equation (3) into (2) can be expressed as equation (4).

$$(R-d)^2 + b^2 = R^2$$
$$d^2 + b^2 = 2Rd \tag{4}$$

Substituting equation (1) into (4), the turning radius R following the path can be obtained as in the following equation (5).

$$R = l^2/2d \tag{5}$$

where l and d mean the look-ahead distance between the USV and the look-ahead point, and the shortest distance to the current USV position and path, respectively.

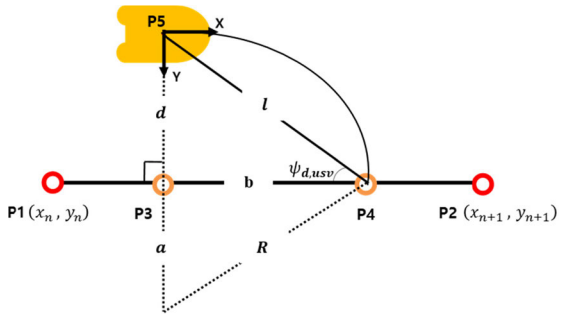

FIGURE 11. Geometry of pure pursuit.

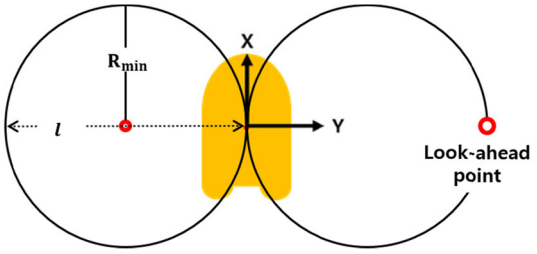

FIGURE 12. Relationship of turning radius and look-ahead distance.

The operator can determine the look-ahead distance l at an arbitrary value, but in this case, the path tracking performance may be degraded, or the USV may move rapidly. Therefore, the look-ahead distance was selected by considering the relationship between the turning radius R and the look-ahead distance l for the USV to approach the reference path.

As shown in figure 12, when the look-ahead point is on the Y-axis of the coordinate system, the turning radius is minimal. Therefore, the minimum turning radius and look-ahead distance can be expressed as equation (6) below.

$$l = 2R_{\min} \tag{6}$$

The minimum turning radius can be checked through the performance test of the USV, and the look-ahead distance can be determined according to equation (6). When the look-ahead distance is determined, the target direction angle that the USV should follow can be obtained using equation (10) using figure 11. At this time P1 and P2 can be obtained from the way points, and P5 from GPS.

$$\psi_{d,usv} = atan2(d, b) \tag{7}$$

B. GEOMETRIC METHOD FOR THE UUV

The UUV tracks the USV while exploring the ocean, and serves to deliver the acquired information in real time. Before platform development, we studied the effect of reducing the underwater cables' impact through a multibody dynamics simulation of the UMV [15]. Our results revealed that the USV and UUV moving with a similar speed in order to maintain a fixed relative formation is effective. Therefore, we tried to follow the USV through relative position and relative heading angle control using USBL and AHRS. For the UUV

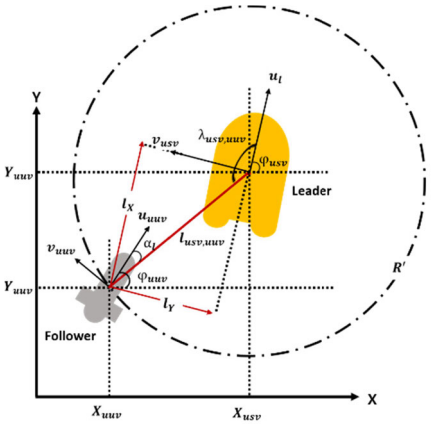

FIGURE 13. Define geometry between the USV and UUV.

to follow the USV, the relative position and relative heading angle were defined as shown in figure 13.

When the UUV is located within the set radius R', the relative position ($l_{usv,uuv}$) and relative heading angle ($\lambda_{usv,uuv}$) expressed in figure 12 can be defined as $l_{usv,uuv} \in \mathbb{R} \geq 0$ and $\lambda_{usv,uuv} \in (\pi/2, 3\pi/2)$, respectively. If the desired relative position and the relative heading angle are $\mathrm{P}^d_{usv,uuv} = [l^d_{usv,uuv}\lambda^d_{usv,uuv}]$, the position and attitude (X_{usv}, Y_{usv}, φ_{usv}) and $\mathrm{P}^d_{usv,uuv} = [l^d_{usv,uuv}, \lambda^d_{usv,uuv}]$ of the USV are known or can be determined, so then the position of the UUV can be uniquely determined. Projecting the relative distance $l_{usv,uuv}$ of the USV and UUV on the X and Y axes is shown in equations (8) and (9) below, and the target distance can be expressed as equations (10) and (11).

$$l_x = -(X_{usv} - X_{uuv})\cos\varphi_{usv} - (Y_{usv} - Y_{uuv})\sin\varphi_{usv} \tag{8}$$

$$l_y = (X_{usv} - X_{uuv})\sin\varphi_{usv} - (Y_{usv} - Y_{uuv})\cos\varphi_{usv} \tag{9}$$

$$l^d_x = l^d_{usv,uuv}\sin(\lambda^d_{usv,uuv} + \varphi_{usv} - \frac{\pi}{2}) \tag{10}$$

$$l^d_y = l^d_{usv,uuv}\cos(\lambda^d_{usv,uuv} + \varphi_{usv} - \frac{\pi}{2}) \tag{11}$$

Finally, the guidance law for the UUV to follow the USV converges the error between the relative distance (l_x, l_y) and the target distance (l^d_x, l^d_y), target relative angle ($\lambda^d_{usv,uuv}$) to zero over time.

On the other hand, if the UUV is outside the range defined byR', the target heading angle is calculated and tracked using relative distance. At this time, the target heading angle is as shown in equation (12).

$$\psi_{d,uuv} = atan2(l_x, l_y) \tag{12}$$

C. ANTI-WINDUP PID CONTROLLER

The Anti-windup PID controller was used to obtain the thruster input to control the USV and UUV. In the case of a general PID controller, the integral controller's value accumulates beyond the limit of the control input of the actual thruster. To determine this, a control method for appropriately limit the value inside the integrator according to the limit value of the controller output was applied [16], [17].

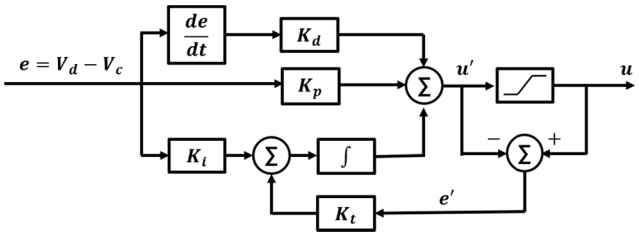

FIGURE 14. Block diagram of the anti-windup PID controller.

TABLE 3. Control target and sensor.

Platform	Control Target	Measurement Sensor
USV	Velocity	GPS
	Heading angle	AHRS
UUV	Relative Position	USBL
	Relative Heading Angle ($< R^{'}$)	USBL
	Heading Angle ($> R^{'}$)	AHRS

Figure 14 shows the block diagram of the anti-windup PID controller.

In figure 14, e represents the difference between the target value and the current value of the control target, and K_p, K_i, K_d and K_t represent the control gains, which were determined through trial and error methods. The control input u can be expressed as equation (13).

$$u = K_p e + K_i \int (e + K_t(sat(u') - u'))dt + K_d \dot{e} \quad (13)$$

Table 3 shows the control targets of the USV and UUV and sensor for measuring the current values. Figure 14 shows the position of the thrusters mounted on the USV and UUV and the notation to distinguish the thrusters.

The USV must control the velocity and heading angle using two thrusters. Therefore, the input of the thruster was determined using the difference of the control input for each control target. The control input of the USV can be expressed as equations (14) and (15).

$$u_{usv,k} = K_{pusv,k} e_k + K_{dusv,k} \dot{e}_k + K_{iusv,k} \int (e_k + K_{tusv,k}(sat(u'_{usv,k}) - u'_{usv,k}))dt \quad (14)$$

$$k = [1, 2] = [velocity_{usv}, heading\ angle_{usv}]$$
$$T_{usv,1} = u_{usv,1} + u_{usv,2}, \quad T_{usv,2} = u_{usv,1} - u_{usv,2} \quad (15)$$

The UUV controls the heading angle using $T_{uuv,3}$ and performs position control using $T_{uuv,1}$, $T_{uuv,2}$. The control input to each thruster can be expressed by the following equations (16), (17) and (18)

$$u_{uuv,j} = K_{puuv,j} e_j + K_{duuv,j} \dot{e}_j + K_{iuuv,j} \times \int (e_j + K_{tuuv,j}(sat(u'_{uuv,j}) - u'_{uuv,j}))dt \quad (16)$$

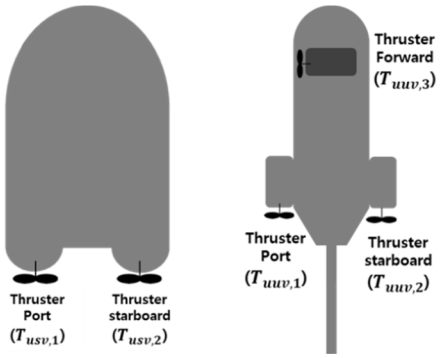

FIGURE 15. Thruster layout of the USV and UUV.

FIGURE 16. Field test scenes of the UMV.

$$j = [1, 2, 3] = [position_{uuv}, relative\ heading\ angle_{uuv}, heading\ angle_{uuv}]$$
$$T_{uuv,1} = T_{uuv,2} = u_{uuv,1} \quad (17)$$
$$if\ position < R', \quad T_{uuv,3} = u_{uuv,2}$$
$$if\ position > R', \quad T_{uuv,3} = u_{uuv,3} \quad (18)$$

IV. FIELD TEST AND RESULTS

In order to confirm the performance of the developed platform and control algorithm, a field tests was conducted. Figure 16 shows the field test scene of the UMV. The experiment was carried out at a yacht mooring station at the Korea Maritime and Ocean University (KMOU). In general, the waypoint tracking control experiment is given as a box and lawnmower type, and the performance can be determined from the experimental results, such as the platform's moving path and heading angle [18]–[20]. In this study, the control performance was further confirmed by using the result for the relative position of the USV and UUV.

The waypoints given for the UMV way point tracking experiment are (50, 0), (50, 50), (0, 50), and (0, 0) including the starting point.

As shown in Figure 17, the USV moves following the given waypoint, and the UUV follows the USV at a displacement of about 3m in the z-axis direction.

Figure 18 shows the heading angles of the USV and UUV while the UMV is performing a waypoint tracking. The black line in the graph represents the heading angle of each platform, and the red line represents the target angle.

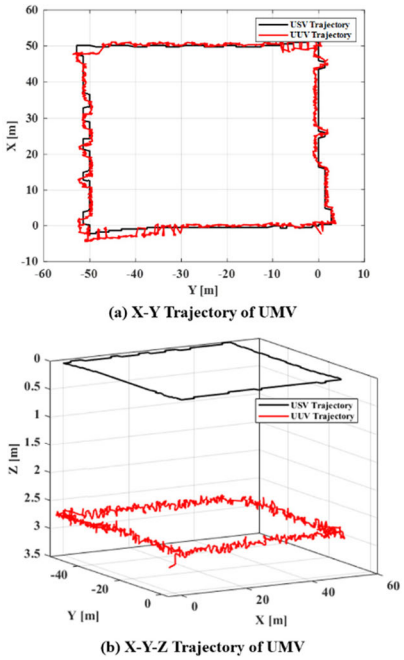

FIGURE 17. Trajectory of the UMV.

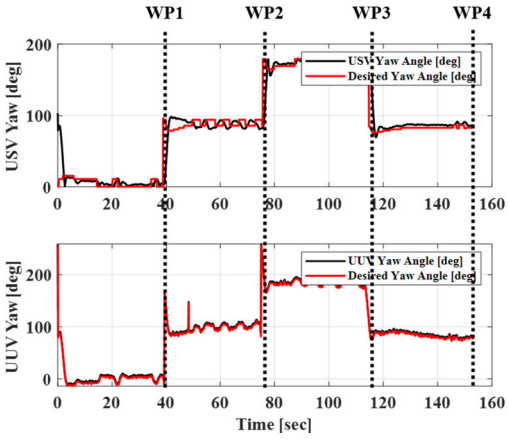

FIGURE 18. Heading angle control result of the USV and UUV.

Although each platform has an error, it continues to follow the target heading angle. The error for the USV may occur because the velocity and heading angle are controlled using two thrusters. In addition, the USV moving at low speed in the water surface may have been affected by disturbances caused by current and waves. Moreover, the UUV follows the value well by performing heading angle control with the thruster in the front, but much overshoot occurs in the section where the target angle changes rapidly.

Figure 19 shows the relative position of the UUV measured using a USBL sensor. The location of the UUV is located in a range smaller than the set effective radius R'. Therefore, we judged that the UUV only controlled the relative heading angle while following the waypoint.

The target moving velocity of the USV is 2m/s, and figure 20 shows the velocity control result. The figure shows,

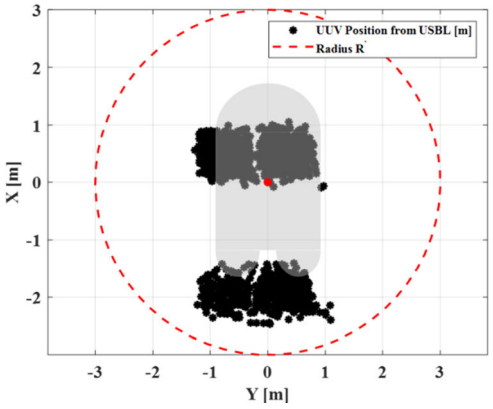

FIGURE 19. Relative position of the UUV w.r.t the USV.

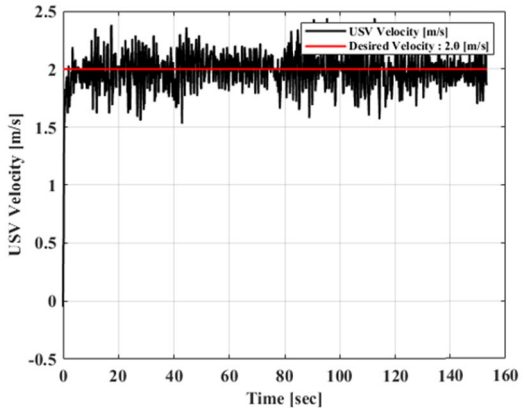

FIGURE 20. Velocity control result of the USV.

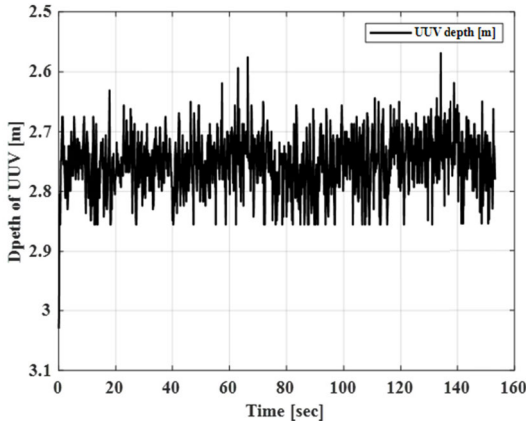

FIGURE 21. Depth of the UUV.

that the USV also moves an average velocity of about 1.98m/s.

The initial UUV was located at a depth of 3m and maintained an average depth of 2.75m while performing waypoint tracking. This result confirmed that the UUV's depth was maintained by using the negative buoyancy at a low speed.

Figure 22 shows the control input of each thruster output through the controller. Through the graph, the change of the

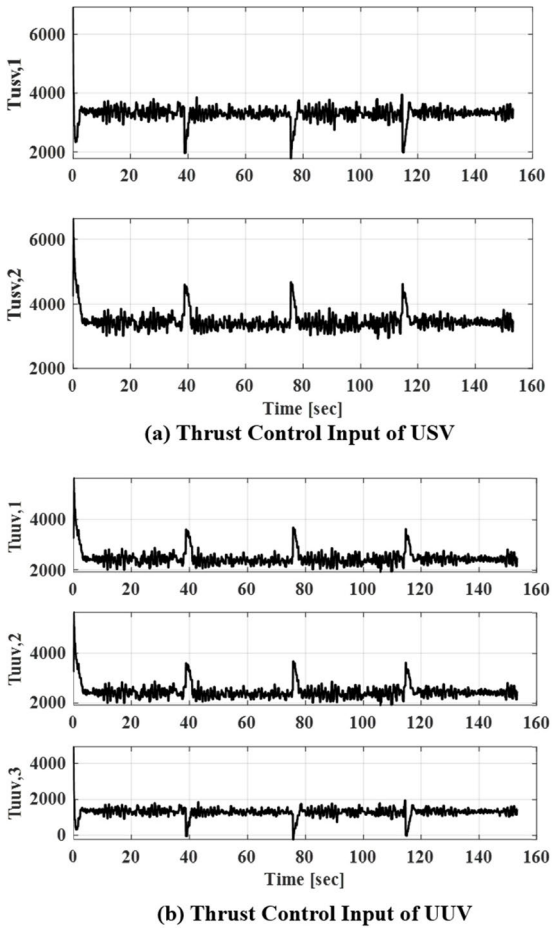

(a) Thrust Control Input of USV

(b) Thrust Control Input of UUV

FIGURE 22. Control input during waypoint tracking.

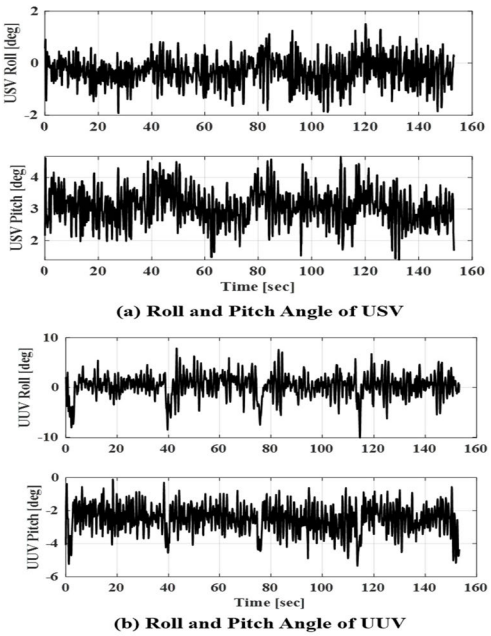

(a) Roll and Pitch Angle of USV

(b) Roll and Pitch Angle of UUV

FIGURE 23. Roll and pitch angle while waypoint tracking.

input value in the section where the waypoint changes can be checked.

Figure 23 shows the attitude values of the USV and UUV while performing waypoint tracking control. The roll and pitch of the USV are −0.31 degrees and 3.2 degrees, respectively. This value varies depending on the sea state, but the experimental value does not significantly affect the motion of the USV. Likewise, the UUV moved with roll and pitch angles of about 0.27 degree and −2.49 degrees, respectively. The UUV roll angle, with a peak of −10.10 degrees, varied significantly in the section where the way point changed.

V. CONCLUSION

This study has introduced a UMV with combined USV and UUV to acquire marine exploration information in real-time. The hardware, electronics, and sensor that make up each platform are described and the algorithm and controller's design process for the controlling the waypoint of the UMV are explained. A field test conducted to check the motion and controller performance of the UMV confirmed that it was moving following a given waypoint, and that there was no problem with the configured hardware and algorithm. The open architecture system for the combined USV and UUV platform will contribute to the development of commercial technology for similar platforms that lack technical information.

Nevertheless other technologies that also need to be studied include a robust controller that can consider the disturbance caused by the underwater cable, obstacle avoidance technology, and the related sensors and algorithms. In line with these requirements, we plan to research an algorithm that combines inertial navigation and a USBL sensor to increase the UUV's positioning accuracy.

REFERENCES

[1] Accessed: Oct. 23, 2020. [Online]. Available: https://www.subsea-tech.com/wpfd_file/brochure-usv-cat-surveyor/
[2] Accessed: Oct. 23, 2020. [Online]. Available: https://www.ecagroup.com/en/business/eca-group-successfully-demonstrates-usv-rov-interoperability-for-subsea-inspections-for-total-and-technipfmc
[3] Accessed: Oct. 23, 2020. [Online]. Available: https://geo-matching.com/usvs-unmanned-surface-vehicles/rsv-sea-observer-usv-with-rov
[4] Accessed: Oct. 23, 2020. [Online]. Available: https://www.textronsystems.com/sites/default/files/_documents/TS%20US%20CUSV%20datasheet.pdf
[5] Accessed: Oct. 23, 2020. [Online]. Available: https://ndiastorage.blob.core.usgovcloudapi.net/ndia/2005/umv_auv/tuesday/mons.pdf
[6] Accessed: Oct. 23, 2020. [Online]. Available: https://oceandiscovery.xprize.org/home
[7] L. Nava-Balanzar, J. L. Sanchez-Gaytán, F. Fonseca-Navarro, T. Salgado-Jiménez, L. G. Garcia-Valdovinos, O. Rubio-Lopez, A. Gómez-Espinosa, and A. Ramirez-Martinez, "Towards teleoperation and automatic control features of an unmanned surface vessel-ROV system: Preliminary results," in *Proc. 14th Int. Conf. Informat. Control, Autom. Robot.*, 2017, pp. 292–299.
[8] V. Djapic and D. Nad, "Using collaborative autonomous vehicles in mine countermeasures," in *Proc. OCEANS IEEE SYDNEY*, May 2010, pp. 1–7.
[9] K. Zwolak, B. Simpson, B. Anderson, E. Bazhenova, R. Falconer, T. Kearns, H. Minami, J. Roperez, A. Rosedee, H. Sade, N. Tinmouth, R. Wigley, and Y. Zarayskaya, "An unmanned seafloor mapping system: The concept of an AUV integrated with the newly designed USV SEA-KIT," in *Proc. OCEANS-Aberdeen*, Jun. 2017, pp. 1–6.
[10] M. G. Fagot, G. J. Moss, D. A. Milburn, and N. H. Gholson, "Deep-towed seismic system design for operation at depths up to 6000m," in *Proc. Offshore Technol. Conf.*, 1981, pp. 853–862.

[11] M. C. Fagot and S. E. Spychalski, "Deep-towed array geophysical system (DTAGS): A hardware description," M.S. thesis, Naval Ocean Res. Devlopment Activity Stennis Space Center, Hancock County, MS, USA, 1984.
[12] E. Borhaug, A. Pavlov, and K. Y. Pettersen, "Integral LOS control for path following of underactuated marine surface vessels in the presence of constant ocean currents," in *Proc. 47th IEEE Conf. Decis. Control*, Dec. 2008, pp. 4984–4991.
[13] S. Yoon, "A simulation study for performance analysis of path tracking method of follow the carrot and pure pursuit," in *Proc. Korean Assoc. Ocean Sci. Technol. Societies Joint Conf.*, 2012, pp. 1582–1585.
[14] D.-H. Kim, C.-J. Kim, and C.-S. Han, "Geometric path tracking and obstacle avoidance methods for an autonomous navigation of nonholonomic mobile robot," *J. Inst. Control, Robot. Syst.*, vol. 16, no. 8, pp. 771–779, Aug. 2010.
[15] S. M. Hong, K. N. Ha, and J.-Y. Kim, "Dynamics modeling and motion simulation of USV/UUV with linked underwater cable," *J. Mar. Sci. Eng.*, vol. 8, no. 5, p. 318, Apr. 2020.
[16] A. Zheng, M. V. Kothare, and M. Morari, "Anti-windup design for internal model control," *Int. J. Control*, vol. 60, no. 5, pp. 1015–1024, Nov. 1994.
[17] M. Kim, H. Joe, J. Pyo, J. Kim, H. Kim, and S.-c. Yu, "Variable-structure PID controller with anti-windup for autonomous underwater vehicle," in *Proc. OCEANS-San Diego*, Sep. 2013, pp. 1–5.
[18] J. Das, F. Py, T. Maughan, T. O'Reilly, M. Messié, J. Ryan, G. S. Sukhatme, and K. Rajan, "Coordinated sampling of dynamic oceanographic features with underwater vehicles and drifters," *Int. J. Robot. Res.*, vol. 31, no. 5, pp. 626–646, Apr. 2012.
[19] K. Rajan, P. Y. Frédéric, and J. Barreiro, "Towards deliberative control in marine robotics," in *Marine Robot Autonomy*. New York, NY, USA: Springer, 2013, pp. 91–175.
[20] Das, Jnaneshwar, "Simultaneous tracking and sampling of dynamic oceanographic features with autonomous underwater vehicles and lagrangian drifters," in *Experimental Robotics*. Berlin, Germany: Springer, 2014.

SUNG MIN HONG (Member, IEEE) was born in Busan, South Korea, in 1988. He received the M.S. degree in mechanical engineering and the Ph.D. degree from the Department of Convergence Study on the Ocean Science and Technology, Graduate School of Ocean Science and Technology, Korea Maritime and Ocean University, Busan, in 2019.

From 2013 to 2019, he was a Research Assistant with the Ship Equipment Design Laboratory. He developed various types of unmanned marine platform, such as manta type AUV, underwater glider, hovering type AUV, and underwater construction robot, and conducted research on dynamic analysis, simulation, and field test. He is currently a member of the Korea Institute of Industrial Technology and works at the Marine Robot Center.

KEON SEOK NAM was born in Ulsan, South Korea, in 1988. He received the B.S. and M.S. degrees in mechanical engineering from Korea Maritime and Ocean University, Busan, South Korea, in 2015.

Since 2015, he has been a Researcher with the Marine Robot Center, Korea Institute of Industrial Technology. He developed underwater glider and hovering type AUV. His interests in underwater navigation and autonomous control.

JE DOO RYU was born in Busan, South Korea, in 1988. He received the M.S. degree in mechanical engineering from Hanyang University, Seoul, South Korea, in 2013.

Since 2013, he has been a Researcher with the Marine Robot Center, Korea Institute of Industrial Technology. His research interests include robot dynamics analysis, structural analysis, and computational fluid dynamics related to marine robot design.

DONG GU LEE was born in Busan, South Korea, in 1979. He received the M.S. degree in intelligent control automation of mechanical engineering and the Ph.D. degree in technology business policy from Pusan National University, Busan, South Korea, in 2014. From 2010 to 2020, he has been working as the Senior Technician with the Marine Robot Center. He supports underwater experiments by underwater robot companies. His research is on ferrofluid simulations and experiments.

KYOUNG NAM HA (Member, IEEE) was born in Busan, South Korea, in 1974. He received the B.S. and Ph.D. degrees in mechanical engineering from Pusan National University, Busan, in 2001 and 2010, respectively. He is currently a Principal Researcher and Chief Officer of the Marine Robot Center, Korea Institute of Industrial Technology, Busan. His research interests are marine robot, remote control systems, and network-based systems.